Iterative rotation scheme for robust dynamical decoupling

Gonzalo A. Álvarez,* Alexandre M. Souza,† and Dieter Suter‡
Fakultät Physik, Technische Universität Dortmund, Dortmund, Germany
(Received 1 March 2012; published 29 May 2012)

The loss of quantum information due to interactions with external degrees of freedom, which is known as decoherence, remains one of the main obstacles for large-scale implementations of quantum computing. Accordingly, different measures are being explored for reducing its effect. One of them is dynamical decoupling (DD) which offers a practical solution because it only requires the application of control pulses to the system qubits. Starting from basic DD sequences, more sophisticated schemes were developed that eliminate higher-order terms of the system-environment interaction and are also more robust against experimental imperfections. A particularly successful scheme, called concatenated DD (CDD), gives a recipe for generating higher-order sequences by inserting lower-order sequences into the delays of a generating sequence. Here, we show how this scheme can be improved further by converting some of the pulses to virtual (and thus ideal) pulses. The resulting scheme, called $(XY4)^n$, results in lower power deposition and is more robust against pulse imperfections than the original CDD scheme.

DOI: 10.1103/PhysRevA.85.052324 PACS number(s): 03.67.Pp, 03.65.Yz, 76.60.Es, 76.60.Lz

I. INTRODUCTION

Quantum information processing (QIP) has acquired a huge interest over the last decades. It can potentially solve many problems qualitatively faster than classical information processing. The quest to implement this scheme has radically improved quantum control technologies (see, e.g., [1]). One of the main remaining obstacles is the sensitivity of quantum systems to interactions with external degrees of freedom that degrade the quantum information [2]. A number of techniques are currently being developed to make reliable quantum computing possible in the presence of environmental noise. A relatively simple technique is dynamical decoupling (DD) [3–15], which uses sequences of control pulses applied to the system qubits. This technique does not require any overhead in terms of ancilla qubits and requires no additional types of control over those that are already needed for information processing. This field has seen significant progress over the last years, and the concept has been demonstrated on a number of different systems [11,16–32].

In the limit of infinitely many ideal refocusing pulses, the DD scheme allows one to completely eliminate the decoherence due to the environmental noise. However, in any real physical implementation, the control pulses necessarily have finite duration and unavoidable imperfections. This leads to a significant reduction of the DD performance, and the effect of a real pulse sequence on the system can actually reduce the fidelity instead of improving it [20,33–40]. Efficient DD schemes must therefore be able to preserve the system fidelity even in the presence of nonideal control fields. An increasing body of research has shown ways towards this goal [20,24,26,35,39,41,42].

One strategy that was shown to be robust against imperfections is a technique called concatenated dynamical decoupling (CDD), which is based on a building block sequence that is concatenated recursively [5,33]. If the delays between the pulses can be reduced indefinitely, CDD was demonstrated to improve its performance with the concatenation order. However, if the delays between the pulses are constrained or the pulses have errors, it was predicted [33] and experimentally demonstrated [20] that an optimal concatenation order exists, and beyond that the DD performance will not improve and may even deteriorate.

To increase the concatenation order, the procedure inserts the lower-order CDD sequence into the delays of the building block sequence. If the pulses have imperfections and the building block sequence compensates partially their effects at the end of the cycle, the CDD sequence will also compensate them at the end of the complete sequence. However, if the average delay between pulses is kept fixed [20,25,26], the duration of the CDD cycle increases exponentially with the CDD order. The compensation of the pulse imperfections only occurs at the end of the cycle. If the cycle time exceeds the correlation time of the environmental fluctuations, this error compensation becomes inefficient and the DD performance decreases.

In this article, we present an approach to the CDD scheme that does not require waiting for the end of the cycle to compensate the pulse imperfections. Instead, they are always compensated over the duration of the lowest-order cycle. This is done by replacing the pulses of the outermost sequence with mathematical operations corresponding to virtual pulses. These virtual pulses are ideal and do not introduce any imperfections. As a result, this method is more robust against pulse imperfections and improves the DD performance significantly. Here, we give a theoretical analysis of this scheme and show experimentally that it performs better than the CDD method when applied to a single qubit interacting with a pure dephasing environment—a typical situation for many QIP implementations [1].

II. THE SYSTEM

We consider a single qubit $\hat{S}$ as the system that is coupled to a bath. The free evolution Hamiltonian is

$$\widehat{\mathcal{H}}_f = \widehat{\mathcal{H}}_{\mathrm{SE}} + \widehat{\mathcal{H}}_E, \tag{1}$$

*gonzalo.alvarez@tu-dortmund.de
†alexandre@e3.physik.uni-dortmund.de
‡dieter.suter@tu-dortmund.de

in a suitable rotating reference frame that is resonant with the system qubit [43]. $\widehat{\mathcal{H}}_E$ is the environment Hamiltonian and

$$\widehat{\mathcal{H}}_{\rm SE} = \sum_{\beta} \left(b_z^{\beta} \hat{E}_z^{\beta} \hat{S}_z + b_y^{\beta} \hat{E}_y^{\beta} \hat{S}_y + b_x^{\beta} \hat{E}_x^{\beta} \hat{S}_x \right) \qquad (2)$$

is a general system-environment (SE) interaction. The operators $\hat{E}_u^{\beta}$ are environment operators and b_u^{β} are the SE coupling strengths. The index β runs over all modes of the environment. Dephasing effects come from the interaction that affects the z component of the spin-system operator, and spin flips and/or polarization damping are produced through the x and/or y operators. We will discuss our method in a general SE interaction context, but the experimental results were performed on a spin system coupled with a spin bath. The SE interaction is given by a heteronuclear spin-spin interaction that effects a pure dephasing. In general, this type of interaction is naturally encountered in a wide range of solid-state spin systems, for example in nuclear magnetic resonance (NMR) [20,25,44,45], electron spins in diamonds [24], electron spins in quantum dots [46], donors in silicon [47], etc. In other cases, when the system and environment have similar energies, the SE interaction can include terms along the x, y, and z axis.

III. CDD WITH REAL AND VIRTUAL PULSES

A. CDD

Concatenated DD (CDD) is a scheme for improving the efficiency of a DD sequence [5,33] by recursively concatenating lower-order sequences CDD_{n-1} into a higher-order sequence CDD_n by inserting CDD_{n-1} blocks into the delays of a generating sequence:

$$\mathrm{CDD}_n = C_n = C_{n-1}\hat{X}C_{n-1}\hat{Y}C_{n-1}\hat{X}C_{n-1}\hat{Y}, \qquad (3)$$

where $C_0 = \tau$ is a free evolution period and $\hat{X}$ and $\hat{Y}$ are π pulses of the generating sequence. $\mathrm{CDD}_1 = C_1 = XY4$ consists of four rotations around the x and y axes. Its pulse sequence is given by $XY4 = \tau$-$\hat{X}$-τ-$\hat{Y}$-τ-$\hat{X}$-τ-$\hat{Y}$. This sequence can decouple SE interactions that include all three components of the system spin operator [3] and it mitigates the effect of pulse errors compared to the older Carr-Purcell-Meiboom-Gill sequence consisting of identical pulses [48]. This can be understood by considering that pulse imperfections convert an Ising-type SE interaction into an effective general SE interaction [20,33,35], which can be partially eliminated by the $XY4$ sequence. In the QIP community, the $XY4$ sequence is usually referred to as periodic dynamical decoupling. Alternatively, we proposed to use the time symmetric version of $XY4$ [48] in the CDD protocol because the resulting CDD(s) sequences are more efficient at supressing decoherence and pulse error effects [26,35,41]. These symmetric sequences can be written as [26,41,48] $XY4(\mathrm{s}) = \tau/2$-$\hat{X}$-τ-$\hat{Y}$-τ-$\hat{X}$-τ-$\hat{Y}$-$\tau/2$ and

$$\mathrm{CDD(s)}_n = C(s)_n = \sqrt{C(s)_{n-1}}\hat{X}C(s)_{n-1}\hat{Y}C(s)_{n-1}\hat{X}C(s)_{n-1}\hat{Y}\sqrt{C(s)_{n-1}}. \qquad (4)$$

The square root $\sqrt{C(s)_n}$ represents half of the cycle. Each level of concatenation reduces the norm of the first nonvanishing term of the Magnus expansion of the previous level, provided that the norm was small enough to begin with [5,33]. This reduction comes at the expense of an increase of the cycle time by a factor of four. The average Hamiltonian can be calculated in the toggling frame. If the pulses generate ideal π rotations, this can be seen as a sign change of different terms of the SE interaction Eq. (2). The top panel of Fig. 1 shows the CDD_2 scheme and it shows the sign changes of the different terms of the SE interaction in the toggling frame. The parameters f_u with $u = x,y,z$ represent the signs of the terms of Eq. (2) that are proportional to $\hat{S}_x$, $\hat{S}_y$, and $\hat{S}_z$, respectively, in the toggling frame.

B. Effect of pulse imperfections in CDD

Since the precision of any real pulse is finite, they generate an evolution that differs from the ideal one. If many pulses are applied in sequence, these errors can accumulate and seriously reduce the fidelity of the evolution [20,26,35–38], unless the sequence of operations is designed in such a way that the errors from different pulses compensate each other [26,35]. One kind of error of nonideal control pulses is their finite duration, which implies a minimum achievable cycle time. The effects introduced by finite pulse lengths have been considered in different theoretical works [4,33,34]. These works predict that high-order CDD sequences can lose their advantages when the delays between pulses or pulse length are strongly constrained. This is because the fundamental frequency $2\pi/\tau_c$, where τ_c is the period of the toggling frame function $f(t)$, is lower for the longer cycle [25]. The efficiency of all DD sequences is reduced if the noise contains frequency components at the resonance frequencies of their filter function [49]. This was demonstrated for Uhrig dynamical decoupling sequences, but the analysis is similar for CDD sequences because the period of the toggling frame sign function f increases with the concatenation order [25].

As shown in Fig. 1, the toggling frame Hamiltonian for one of the components is not affected by the pulses of the generating sequence (marked by circles). Due to the finite duration of the pulses, this represents an additional contribution to the average Hamiltonian, which is only compensated by the second pulse of the generating sequence with the same rotation axis half a period later. Full compensation of these additional terms is achieved at the end of the complete (higher-order) cycle.

Generally more important than their finite duration are imperfections of the pulses. In most cases, the dominant cause of errors is a deviation between the ideal and the actual

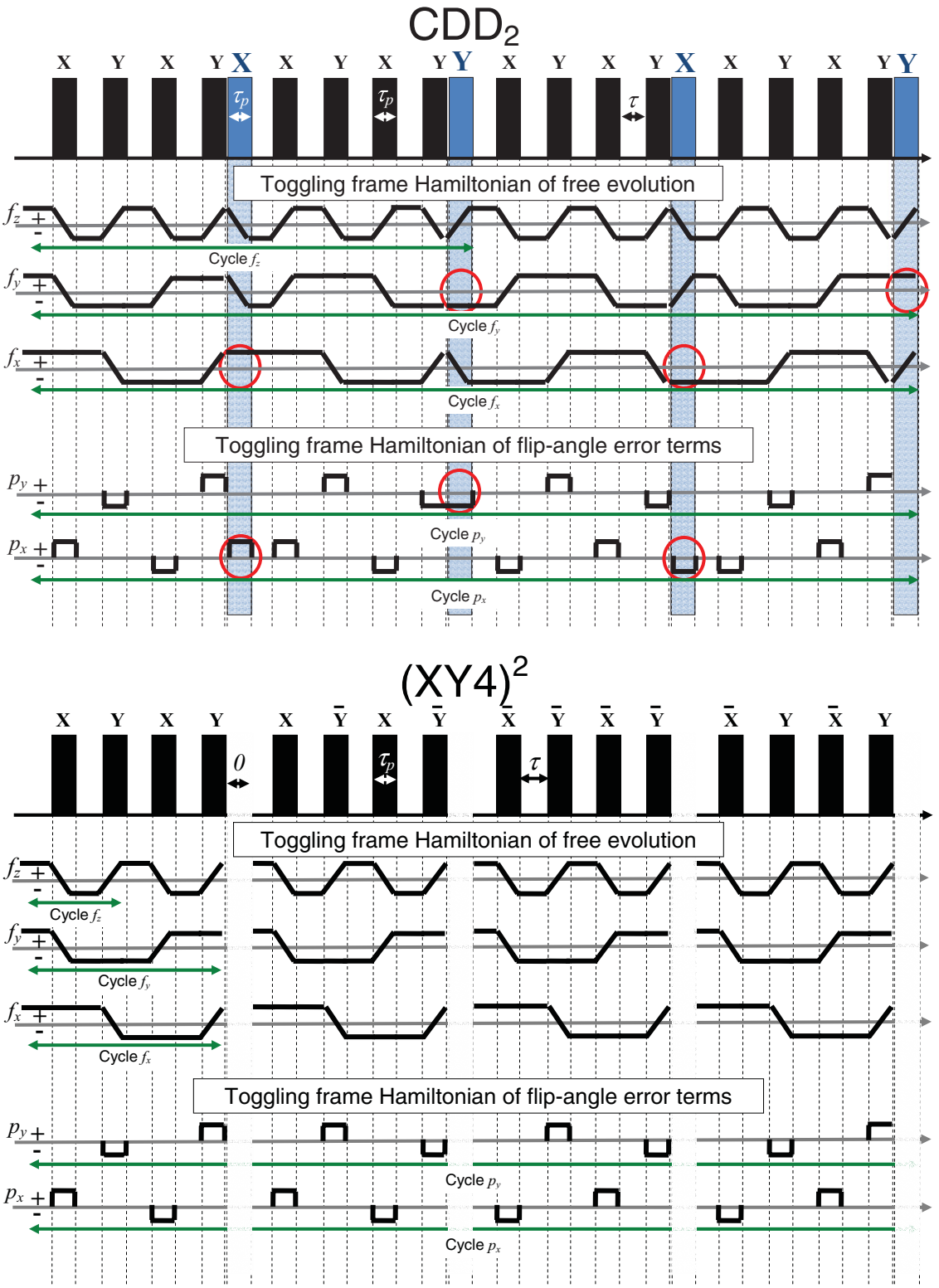

FIG. 1. (Color online) CDD_2 and $(XY4)^2$ pulse sequence schemes. The black solid boxes represent the DD π pulses of the inner sequences with their respective phases. The gray (blue) boxes are the π pulses of the generating sequence for CDD, while for $(XY4)^2$ they are virtual and appear as a transparent white stripe of zero duration. The toggling frame Hamiltonians are represented by the respective signs of the different terms proportional to the $\hat{S}_x$, $\hat{S}_y$, and $\hat{S}_z$ components. Sign changes during the pulses are represented by diagonal lines \ or /. In the CDD_2 scheme, the terms marked by circles are compensated only at the end of the complete cycle, but the $(XY4)^2$ scheme compensates all terms over the basic four-pulse cycle. The toggling frame Hamiltonians of the free evolution interaction for $(XY4)^2$ are the same for all blocks of the inner sequence, i.e., equal to those of the $XY4$ sequence. The toggling frame Hamiltonian of the flip-angle error terms of $(XY4)^2$ is equal to that of the CDD scheme with ideal pulses.

amplitude of the control fields. This results in a rotation angle that deviates from π, typically by a few percent. The propagator for the π pulses including this error is $e^{-i(\pi+\Delta\omega_p\tau_p)\hat{S}_\phi}$, where $\Delta\omega_p$ is the error on the control field amplitude. In the toggling frame Hamiltonian, the ideal part of this propagator, $e^{-i\pi\hat{S}_\phi}$, vanishes, but the error term $e^{-i\Delta\omega_p\tau_p\hat{S}_\phi}$ remains and contributes to the average Hamiltonian. The signs of these terms in the toggling frame are represented as p_u in Fig. 1.

Another important error occurs when the control field is not applied on resonance with the transition frequency of the qubit. This off-resonance error adds a term $f_z\Delta_z\hat{S}_z$ to the toggling frame Hamiltonian.

The $XY4$ sequence cancels these errors in zeroth order, independent of the initial condition [48,50]. As a result, the performance of this sequence is quite symmetric with respect to the initial state in the x-y plane and the average decay times are significantly longer than with nonrobust sequences [20,24,26,35]. The concatenation scheme proposed by Khodjasteh and Lidar [5,33] improves the decoupling performance and the tolerance to pulse imperfections [20,26]. However, the finite duration of the pulses and constrained delays between pulses result in the existence of optimal levels of concatenation [20,26], with decreasing performance for higher-level sequences. This can be seen in Fig. 2, where decay curves are plotted for different DD sequences, including the free evolution decay, the Hahn echo decay [51], and different orders of CDD for their optimal delay between pulses. Panel (b) shows the decay times for different CDD sequences and delays τ between pulses. For each sequence, the decoherence time reaches a maximum; for delays shorter than the optimal value, the pulse errors dominate. The relation between the optimal delay time and its CDD order is plotted in the inset of Fig. 2(b). The experimental dependence agrees remarkably well with the predicted curve [33].

C. CDD with virtual pulses

In Ref. [20], we suggested to improve the concatenation scheme by compensating the pulse errors of the generating sequence [gray (blue) boxes, Fig. 1] before the end of the complete cycle. Looking into the details of the toggling frame Hamiltonians, we can see that at each concatenation level of the $XY4$ generating sequence [gray (blue) boxes in the top panel of Fig. 1] additional pulse errors are introduced that are only compensated at the end of the complete cycle. As a result, the properties of the real CDD sequence deviate strongly from those of the ideal sequence.

Here, we show how these additional pulse errors can be completely avoided by using virtual (and thus ideal) rotations for the generating sequence instead of the real ones. To motivate the idea, we consider the first pulse of the generating sequence and the subsequent pulses of the cycle from the lower-order sequence. The corresponding evolution operator can be written

$$\ldots(\hat{Y}\hat{X}\hat{Y}\hat{X})\hat{X}\ldots = \ldots\hat{X}(\hat{\bar{Y}}\hat{X}\hat{\bar{Y}}\hat{X})\ldots, \tag{5}$$

where the pulse sequence is read from right to left. The bar over X and Y means that the sense of rotation is reversed for those pulses. The second form corresponds to a modified $XY4$ cycle, followed by the π_x pulse of the generating sequence. In the modified cycle, the direction of rotation of the y pulses has been inverted. We distinguish this modified cycle from the original cycle by writing them as $X\bar{Y}4$ and $XY4$, respectively. Similarly, the subsequent cycles become $\bar{X}\bar{Y}4$

$$\ldots(\hat{Y}\hat{X}\hat{Y}\hat{X})\hat{Y}\hat{X}\ldots = \ldots\hat{Y}\hat{X}(\hat{\bar{Y}}\hat{\bar{X}}\hat{\bar{Y}}\hat{\bar{X}})\ldots \tag{6}$$

and $\bar{X}Y4$

$$\hat{Y}(\hat{Y}\hat{X}\hat{Y}\hat{X})\hat{X}\hat{Y}\hat{X}\ldots = \hat{Y}\hat{X}\hat{Y}\hat{X}(\hat{Y}\hat{\bar{X}}\hat{Y}\hat{\bar{X}})\ldots. \tag{7}$$

As the pulses of the generating sequence are thus moved to the end of the cycle, they cancel ($\hat{Y}\hat{X}\hat{Y}\hat{X} = \hat{1}$) and can be omitted

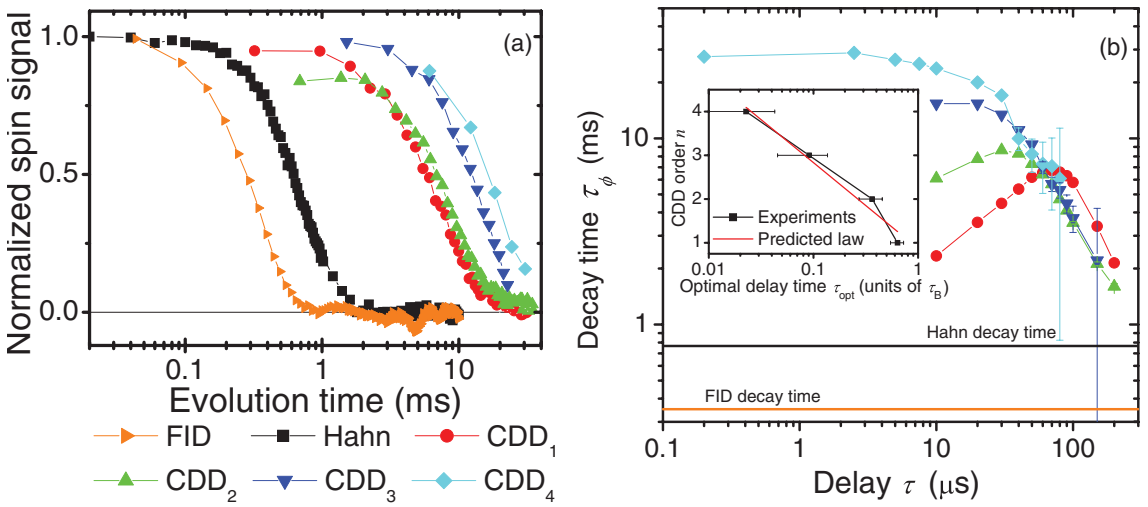

FIG. 2. (Color online) Decays of coherence under the influence of different DD sequences. (a) Normalized spin signal decay of the echo trains of different CDD sequences, the Hahn echo decay [51], and the free evolution (FID). The CDD decay curves are plotted for their optimal delays between pulses that are given when the curves of panel (b) have a maximum. (b) Decay times of different CDD sequences for different delays between pulses. The optimal delay time is defined when the decay is a maximum. Inset: dependence as a function of the CDD order matching with theoretical predictions [33]. $\tau_B = 110\ \mu$s is the bath correlation time [20].

completely. In this sense, we have replaced these pulses by "virtual pulses" corresponding to phase changes of the pulses in the inner sequence. The resulting sequence, which is shown in Fig. 1, can be written recursively as

$$(XY4)^1 = XY4, \tag{8}$$

$$(XY4)^n = (XY4)^{n-1}\text{-}(X\bar{Y}4)^{n-1}\text{-}(\bar{X}\bar{Y}4)^{n-1}\text{-}(\bar{X}Y4)^{n-1}. \tag{9}$$

This scheme represents the time symmetric as well as the asymmetric version, which differ only by the duration of the free precession periods at the beginning and end of the full cycle.

As shown in Fig. 1, the toggling frame Hamiltonian generated by this sequence differs from that of the original CDD sequence. As shown in the lower part of the figure, the function f has for each four-pulse block the same time dependence as for the $XY4$ sequence. The terms marked by circles in the upper part of the figure are missing in the lower part; accordingly, the average of the f_u vanishes over each block of the inner sequence. Similarly, the pulse error contributions p_u do not have contributions from the generating sequence and therefore also compensate over each lower-order cycle. In the lowest-order average Hamiltonian, the $(XY4)^n$ sequences therefore compensate all errors over a single $XY4$ cycle, while the corresponding time for CDD_n is 4^n times longer. For the $(XY4)^n$ sequence, the lowest frequency of the filter function is therefore always $2\pi/\tau_1$, where τ_1 is the duration of the $\mathrm{CDD}_1 = XY4$ cycle. In contrast to that, the fundamental frequency of the CDD_n sequence decreases with $1/4^n$, which can make it sensitive to low-frequency noise with high amplitudes, such as frequency offsets and errors of control fields.

The change in the toggling frame Hamiltonian effected by the pulses of the generating sequence of CDD can of course also be a desired property, since it compensates higher-order terms of the average Hamiltonian, including cross terms between pulse imperfections and environmental contributions. Some of these effects are also present in the $(XY4)^n$ scheme, since the nonvanishing higher-order average Hamiltonians of the different blocks are not identical. The concatenation scheme is designed to compensate them over the full cycle. A detailed discussion of these higher-order contributions is beyond the scope of this paper and probably not feasible without considering specific system parameters. Instead, we compare the two schemes experimentally.

IV. EXPERIMENTAL PERFORMANCE COMPARISON

A. System and setup

We experimentally implemented the new $(XY4)^n$ scheme and compared its performance to that of the CDD scheme. The experiments were performed on a polycrystalline adamantane sample using a home-built solid-state NMR spectrometer with a ^{1}H resonance frequency of 300 MHz. Our system qubits are the ^{13}C nuclear spins of the adamantane molecule, which contains two nonequivalent carbon atoms. Under our conditions, they have similar dynamics. Here, we present the results from the CH_2 carbon. Working with a natural abundance sample (1.1% ^{13}C), the interaction between the ^{13}C-nuclear spins can be neglected. The main mechanism for decoherence is the interaction with the neighboring proton spins. As discussed before, this interaction generates pure dephasing. This interaction is not static, since the dipole-dipole couplings within the proton bath cause flip-flops of the protons coupled to the carbon. The π pulses for DD were applied on resonance with the ^{13}C spins. Their radio-frequency (RF) field of $\approx 2\pi \times 50$ kHz gives a π-pulse length τ_p between 10 and 10.6 μs. The measured RF field inhomogeneity was about 10%.

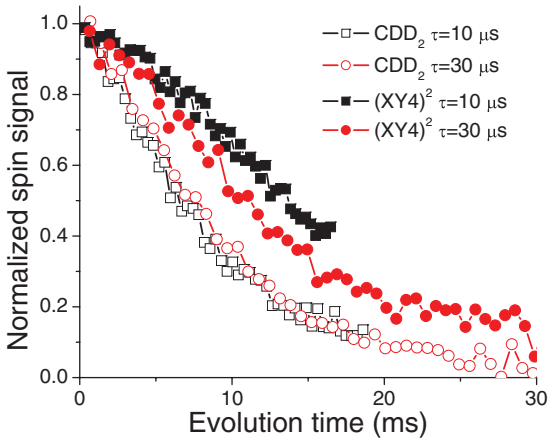

FIG. 3. (Color online) Normalized spin signal decays for $(XY4)^2$ and CDD_2 for different delays τ.

B. $(XY4)^n$ and CDD under optimal conditions

Figure 3 compares the decay of the spin signal for the asymmetric versions of CDD_2 and $(XY4)^2$ for two different pulse spacings τ. For the $(XY4)^2$ sequence, the decay is clearly slower; the $1/e$ decay times are 17 and 14.6 ms for the two delays, compared to 8.9 and 10.1 ms for the CDD_2 sequence.

Figure 4 shows the decay times for different asymmetric CDD and $(XY4)^n$ orders obtained for different duty cycles, i.e., the ratio between the irradiation time $N_p\tau_p$ over the total time $(N_p\tau_p + N\tau)$, where N_p is the number of pulses in a cycle and N is the number of delays. τ_p was kept fixed and we varied the delay τ between the pulses. Comparing the curves for the

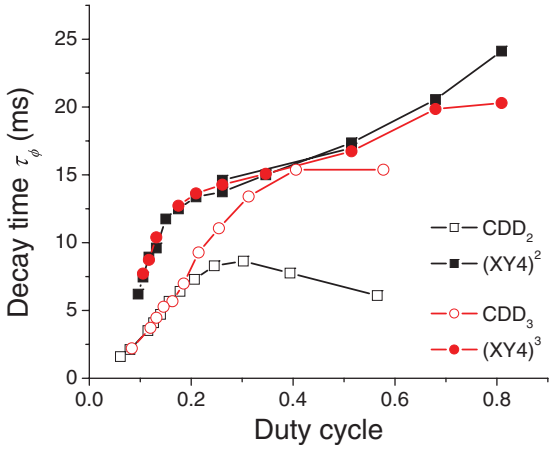

FIG. 4. (Color online) Decay times for $(XY4)^n$ and CDD_n of order 2 and 3 as a function of the duty cycle.

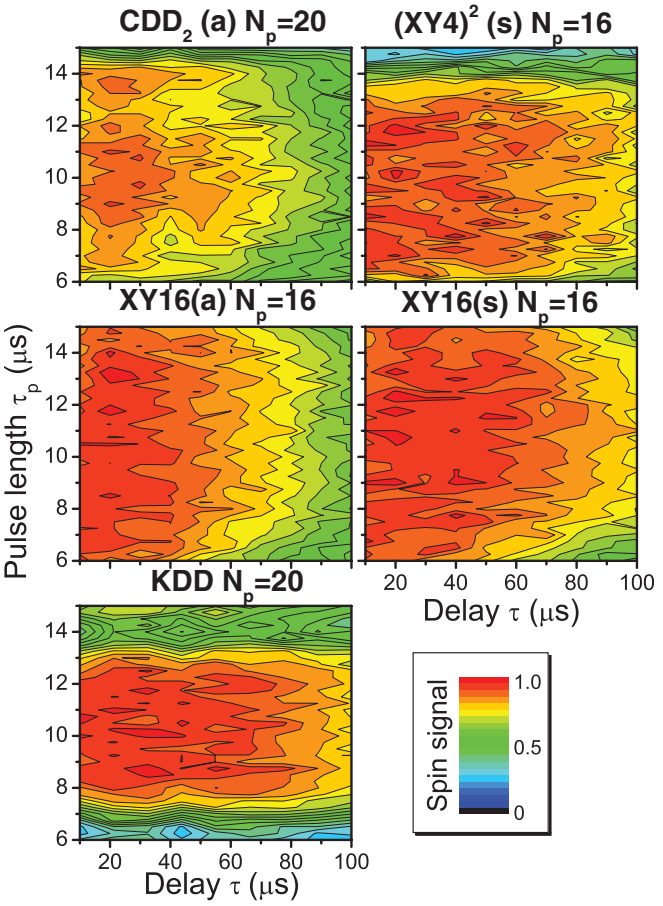

FIG. 5. (Color online) Normalized spin signal after one cycle of different DD sequences as a function of the pulse length of the DD pulses and the delay between them. The labels (a) and (s) refer to the asymmetric and symmetric versions of the sequences.

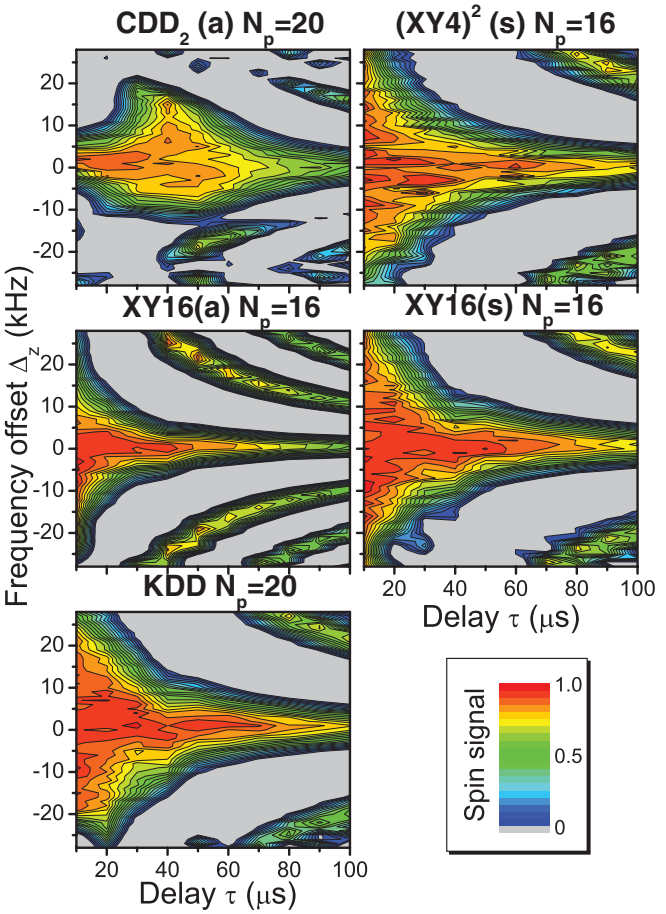

FIG. 6. (Color online) Normalized spin signal after one cycle of different DD sequences as a function of the offset frequency of the DD pulses and the delay between them. The labels (a) and (s) refer to the asymmetric and symmetric versions of the sequences.

two schemes, we find that $(XY4)^n$ performs better than the CDD sequences for all duty cycles (delays). While the CDD performance changes as a function of the order, the difference between the two $(XY4)^n$ sequences is not significant. The difference between the symmetric and asymmetric version of $(XY4)^n$ also was not significant. This suggests that the second order achieves already the optimal DD performance for our experimental conditions. The observed performance is also very similar to that of the KDD [26] sequence measured in an earlier study (Sec. V for details). Both the $(XY4)^n$ and the CDD sequences perform symmetrically for initial conditions in the x-y plane.

C. Effect of pulse errors

Under normal experimental conditions, we cannot see any difference between the $(XY4)^n$ scheme and other robust sequences like KDD and $XY16$ [20,26,35,41]. For a quantitative comparison of their robustness we also tested the performance of the sequences against artificially added pulse errors. We compared CDD_n with $(XY4)^n$ and with the optimal sequences obtained in previous works, i.e., $XY16$ and KDD [26,35,41]. Figures 5 and 6 compare the spin signal after one cycle of the respective sequence for different pulse errors. Figure 5 shows the surviving spin polarization as a function of the pulse duration (and thus of the flip angle) and the delay between the pulses. The number of pulses per cycle is not exactly the same for the different sequences [16 for $(XY4)^2$ and $XY16$ versus 20 for CDD_2 and KDD], but we consider this to be sufficiently similar to allow a rough comparison. For all sequences, there is little correlation between the flip-angle error and the delay between the pulses. This is a consequence of the fact that the terms in the propagator that involve the flip-angle error are proportional to the pulse width τ_p but independent of the pulse separation τ.

Figure 6 shows similar data, but here we introduced an artificial offset error Δ_z rather than a flip-angle error. In this case, there is a strong correlation between the effect of the offset and the delay between the pulses. This is expected, because an offset error generates an extra dephasing term in the propagator that generates an additional precession by an angle $\Delta_z\tau$. Without the SE interaction or another source of errors (like flip-angle error inhomogeneity), we do not expect a significant dependence on τ, because the offset is static and can be completely refocused with DD. Our real system has a bath correlation time of $\approx$100 μs [20,25], which explains the observed decay for cycle times of this order.

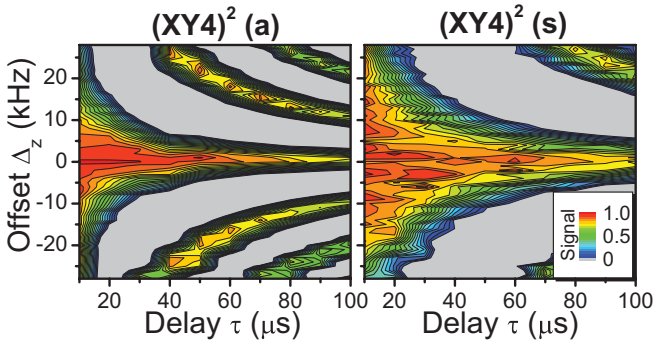

FIG. 7. (Color online) Normalized spin signal after one cycle for the symmetric (s) and asymmetric (a) version of $(XY4)^2$ as a function of the offset frequency of the DD pulses and the delay between them. Both sequences have the same number of pulses and cycle time.

Comparing the standard CDD_2 with the symmetric version of $(XY4)^2$ in Figs. 5(a) and 5(b), we can see that the overall performance of $(XY4)^2$ is better than that of CDD, as expected by the analysis of Sec. III. This is because $(XY4)^2$ is more effective in compensating the flip-angle errors. $(XY4)^2$ also outperforms CDD in the presence of offset errors [see Figs. 6(a) and 6(b)]. Comparing the asymmetric and symmetric version of $(XY4)^2$ as a function of flip-angle error, we observe no significant differences. However, $(XY4)^2$(s) clearly outperforms $(XY4)^2$(a) in the presence of offset errors (Fig. 7). Comparing against the other sequences, $(XY4)^2$ seems to perform better than KDD as a function of flip-angle errors. The good performance of $XY16$ is expected because its evolution operators (symmetric and asymmetric) are equal to the identity operator as long as spin-bath effects are absent: the sequence is designed to generate a propagator $UU^{\dagger}$, independent of flip-angle errors. For small delays between pulses, $XY16$ is the most robust sequence as a function of flip-angle error. Its symmetric version performs slightly better than the asymmetric version. As a function of offset error, $(XY4)^2$(s), KDD, and $XY16$(s) behave similarly and they are more robust than $(XY4)^2$(a) and $XY16$(a). Note that the behaviors of the asymmetric version of $(XY4)^2$ and $XY16$ as a function of offset errors are also similar.

To amplify the effect of pulse imperfections, we also performed experiments with ≈100 pulses as a function of the delay between the pulses and added specific pulse imperfections (Figs. 8 and 9). Under these conditions, also the accumulated exposure to the spin bath is longer. Clearly now

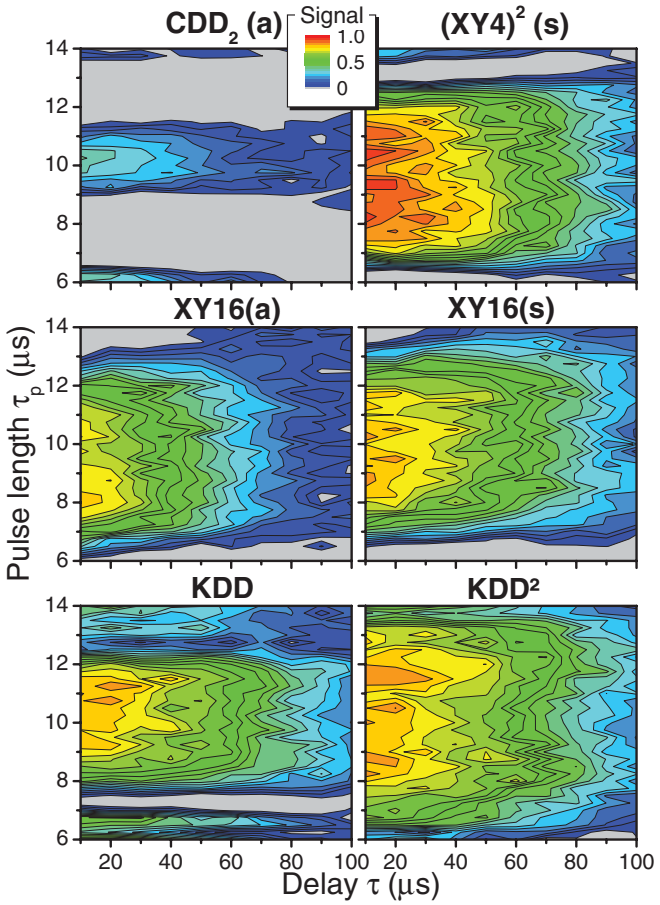

FIG. 8. (Color online) Normalized spin signal after about 100 pulses for different DD sequences as a function of the pulse length of the DD pulses and the delay between them. All sequences have 100 pulses except $(XY4)^2$, which contains 96. The labels (a) and (s) refer to the asymmetric and symmetric version of the sequences.

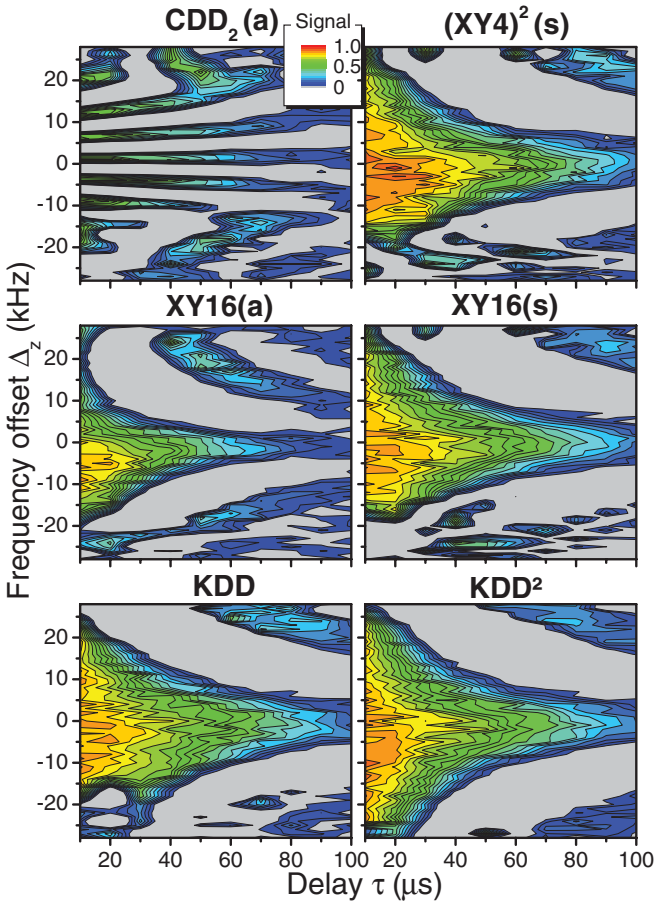

FIG. 9. (Color online) Normalized spin signal after about 100 pulses for different DD sequences as a function of the offset frequency of the DD pulses and the delay between them. All sequences have 100 pulses except $(XY4)^2$, which contains 96. The labels (a) and (s) refer to the asymmetric and symmetric version of the sequences.

the $(XY4)^2$ sequence outperforms always the CDD version for every condition. As a function of flip-angle error, the performance of $(XY4)^2$(s) and $(XY4)^2$(a) is comparable [$(XY4)^2$(a) is not shown]. The $(XY4)^2$ performance as a function of flip-angle error is even better than KDD and comparable to $XY16$(s). As a function of offset error, the performance of $(XY4)^2$(s) is comparable to KDD and $XY16$(s); however, in this case $(XY4)^2$(a) is less robust (not shown in the figure).

V. OTHER GENERATING SEQUENCES

The concept introduced here can not only be applied to the $XY4$ sequence but also to other generating sequences, such as the KDD sequence [26]. KDD was inspired from a sequence of adjacent π pulses that combine to a robust π pulse [52]:

$$\Pi_\phi = \pi_{\phi+30} - \pi_{\phi+0} - \pi_{\phi+90} - \pi_{\phi+0} - \pi_{\phi+30}. \tag{10}$$

The decoupling sequence is obtained first by introducing delays between the individual pulses [26]:

$$\Pi_\phi(\tau)$$
$$f_{\tau/2}\text{-}\pi_{\phi+30}\text{-}f_\tau\text{-}\pi_{\phi+0}\text{-}f_\tau\text{-}\pi_{\phi+90}\text{-}f_\tau\text{-}\pi_{\phi+0}\text{-}f_\tau\text{-}\pi_{\phi+30}\text{-}f_{\tau/2}. \tag{11}$$

The lower indexes denote the pulse phase, i.e., the orientation of the rotation axes in the x-y plane. If we use $XY4$ as the (virtual) generating sequence and $\Pi_\phi(\tau)$ as building blocks, we arrive at

$$\mathrm{KDD} = \Pi_X(\tau) - \Pi_Y(\tau) - \Pi_X(\tau) - \Pi_Y(\tau), \tag{12}$$

which we introduced and tested in [26].

If we use the sequence Eq. (10) instead of $XY4$ as the (virtual) generating sequence, we obtain a new sequence:

$$\mathrm{KDD}^2 = [\Pi_{30}(\tau) - \Pi_0(\tau) - \Pi_{90}(\tau) - \Pi_0(\tau) - \Pi_{30}(\tau)]^2 .$$

As indicated by the square after the bracket, the complete cycle consists of 50 pulses. Iterations to higher order are of course possible but will not be covered here.

In Figs. 8 and 9, we also show the experimental performance of this new sequence, together with the sequences discussed earlier. We clearly see that this new sequence is extremely robust and outperforms all other sequences.

VI. CONCLUSIONS

We have presented an iterative method for generating robust sequences for dynamical decoupling: for the generating sequence, we use virtual rotations instead of physical control operations. Since these rotations are ideal, our scheme avoids introducing additional pulse imperfections, reduces the power deposition on the system, and makes the resulting sequences more robust. As a result of the reduced number of control operations, the toggling frame Hamiltonian has a different time dependence than in the CDD scheme. We have tested two different expansion schemes based on these virtual rotations, called $(XY4)^n$ and KDD^2. Both types of sequences have proved to be very robust under our experimental conditions. It will be interesting to see if these results can be reproduced in other systems.

ACKNOWLEDGMENTS

We acknowledge discussion with Daniel Lidar and Gregory Quiroz. This work is supported by the Deutsche Forschungsgemeinschaft through Grant No. Su 192/24-1.

[1] T. D. Ladd, F. Jelezko, R. Laflamme, Y. Nakamura, C. Monroe, and J. L. O'Brien, Nature (London) **464**, 45 (2010).
[2] W. Zurek, Rev. Mod. Phys. **75**, 715 (2003).
[3] L. Viola, E. Knill, and S. Lloyd, Phys. Rev. Lett. **82**, 2417 (1999).
[4] L. Viola and E. Knill, Phys. Rev. Lett. **90**, 037901 (2003).
[5] K. Khodjasteh and D. A. Lidar, Phys. Rev. Lett. **95**, 180501 (2005).
[6] G. S. Uhrig, Phys. Rev. Lett. **98**, 100504 (2007).
[7] G. Gordon, G. Kurizki, and D. A. Lidar, Phys. Rev. Lett. **101**, 010403 (2008).
[8] G. S. Uhrig, Phys. Rev. Lett. **102**, 120502 (2009).
[9] J. R. West, B. H. Fong, and D. A. Lidar, Phys. Rev. Lett. **104**, 130501 (2010).
[10] K. Khodjasteh, D. A. Lidar, and L. Viola, Phys. Rev. Lett. **104**, 090501 (2010).
[11] J. Clausen, G. Bensky, and G. Kurizki, Phys. Rev. Lett. **104**, 040401 (2010).
[12] W. Yang, Z. Wang, and R. Liu, Front. Phys. **6**, 2 (2010).
[13] Z. Y. Wang and R. B. Liu, Phys. Rev. A **83**, 022306 (2011).
[14] G. Quiroz and D. A. Lidar, Phys. Rev. A **84**, 042328 (2011).
[15] W. J. Kuo and D. A. Lidar, Phys. Rev. A **84**, 042329 (2011).
[16] L. Cywinski, R. M. Lutchyn, C. P. Nave, and S. DasSarma, Phys. Rev. B **77**, 174509 (2008).
[17] W. Yang and R. B. Liu, Phys. Rev. Lett. **101**, 180403 (2008).
[18] M. J. Biercuk *et al.*, Nature (London) **458**, 996 (2009).
[19] J. Du *et al.*, Nature (London) **461**, 1265 (2009).
[20] G. A. Álvarez, A. Ajoy, X. Peng, and D. Suter, Phys. Rev. A **82**, 042306 (2010).
[21] G. de Lange, Z. H. Wang, D. Riste, V. V. Dobrovitski, and R. Hanson, Science **330**, 60 (2010).
[22] C. Barthel, J. Medford, C. M. Marcus, M. P. Hanson, and A. C. Gossard, Phys. Rev. Lett. **105**, 266808 (2010).
[23] S. Pasini and G. S. Uhrig, Phys. Rev. A **81**, 012309 (2010).
[24] C. A. Ryan, J. S. Hodges, and D. G. Cory, Phys. Rev. Lett. **105**, 200402 (2010).
[25] A. Ajoy, G. A. Álvarez, and D. Suter, Phys. Rev. A **83**, 032303 (2011).
[26] A. M. Souza, G. A. Álvarez, and D. Suter, Phys. Rev. Lett. **106**, 240501 (2011).
[27] I. Almog, Y. Sagi, G. Gordon, G. Bensky, G. Kurizki, and N. Davidson, J. Phys. B **44**, 154006 (2011).
[28] B. R. Bardhan, P. M. Anisimov, M. K. Gupta, N. C. Jones, H. Lee, and J. P. Dowling, e-print arXiv:1105.4164 (2011).
[29] Y. Pan, Z. Xi, and J. Gong, J. Phys. B **44**, 175501 (2011).

[30] A. Shukla and T. S. Mahesh, e-print arXiv:1110.1473 (2011).
[31] H. Bluhm, S. Foletti, I. Neder, M. Rudner, D. Mahalu, V. Umansky, and A. Yacoby, Nat. Phys. **7**, 109 (2011).
[32] B. Naydenov, F. Dolde, L. T. Hall, C. Shin, H. Fedder, L. C. L. Hollenberg, F. Jelezko, and J. Wrachtrup, Phys. Rev. B **83**, 081201 (2011).
[33] K. Khodjasteh and D. A. Lidar, Phys. Rev. A **75**, 062310 (2007).
[34] T. E. Hodgson, L. Viola, and I. D'Amico, Phys. Rev. A **81**, 062321 (2010).
[35] A. M. Souza, G. A. Álvarez, and D. Suter [accepted in Phil. Trans. R. Soc. A (2012)], e-print arXiv:1110.6334 (2011).
[36] Z. Wang and V. V. Dobrovitski, J. Phys. B **44**, 154004 (2011).
[37] Z. Xiao, L. He, and W.-g. Wang, Phys. Rev. A **83**, 032322 (2011).
[38] Z. Wang, W. Zhang, A. M. Tyryshkin, S. A. Lyon, J. W. Ager, E. E. Haller, and V. V. Dobrovitski, Phys. Rev. B **85**, 085206 (2012).
[39] K. Khodjasteh, T. Erdélyi, and L. Viola, Phys. Rev. A **83**, 020305 (2011).
[40] X. Peng, D. Suter, and D. A. Lidar, J. Phys. B **44**, 154003 (2011).
[41] A. M. Souza, G. A. Álvarez, and D. Suter, Phys. Rev. A **85**, 032306 (2012).
[42] J. M. Cai, F. Jelezko, M. B. Plenio, and A. Retzker, e-print arXiv:1111.0930 (2011).
[43] A. Abragam, *Principles of Nuclear Magnetism* (Oxford University Press, London, 1961).
[44] H. Y. Carr and E. M. Purcell, Phys. Rev. **94**, 630 (1954).
[45] S. Meiboom and D. Gill, Rev. Sci. Instrum. **29**, 688 (1958).
[46] R. Hanson *et al*., Rev. Mod. Phys. **79**, 1217 (2007).
[47] B. E. Kane, Nature (London) **393**, 133 (1998).
[48] A. A. Maudsley, J. Magn. Reson. **69**, 488 (1986).
[49] G. A. Álvarez and D. Suter, Phys. Rev. Lett. **107**, 230501 (2011).
[50] T. Gullion, D. B. Baker, and M. S. Conradi, J. Magn. Reson. **89**, 479 (1990).
[51] E. L. Hahn, Phys. Rev. **80**, 580 (1950).
[52] R. Tycko, A. Pines, and J. Guckenheimer, J. Chem. Phys. **83**, 2775 (1985).